Impact Analysis of Thin Shell Structure: Verification of AUTODYN-2D with Experimental Data

M. Katayama
Century Research Center Corporation, Tokyo, Japan
T. Aizawa
University of Tokyo, Tokyo, Japan

1. INTRODUCTION

In the field of safety engineering for nuclear structures or components, impact analysis codes have been utilized to understand how the mechanical behaviors in scenario would take place in experimental and actual situations. Some of dynamic analysis programs have been applied to materials forming in order to predict the final geometry and dimensions of workpiece through high-energy forming. Since the accuracy and validity of thus obtained nonlinear solutions is completely dependent on the employed algorithms and modelings in programs, many engineers are urgently required to comprehend the accuracy and reliability of impact analysis.

In the present paper, a standard problem is selected to verify numerical approach by the experimental data and to make some evaluations on the numeriacl modelings. The reference experiments were performed for thin annular lead diaphragms by using an inertial forming machine with impulse velocities, from 3.5 m/sec through 23.5 m/sec. As a computational simulator, the thin shell processor of AUTODYN-2D is employed: with respect to material model, the strain-rate dependency of lead is taken into account.

Although the present study is confined to a thin metal sheet forming, we are sure to make a contribution toward general impact analysis of thin structures appearing in the missile impact, cask drop and explosive forming processes.

2. SIMULATOR

AUTODYN-2D (Birnbaum et al, 1987; Itoh et al, 1987) is a two dimensional non-linear dynamic analysis program on the basis of the well proven Lagrangian and Eulerian finite difference techniques. The current version of this program enables us to select four different processors for each problem we are facing: a Lagrange processor, an Euler processor, an ALE processor, and a shell processor. The Lagrange processor was verified (Birnbaum et al, 1987) for a missile impact problem compared with experiment. Then this verification of the shell processor, which is useful and efficient for thin structures, will extend its application area considerably.

3. REFERENCE EXPERIMENTS

A series of experiments on annular diaphragms (Ghosh et al, 1985) were carried out by using an inertial forming machine. Fig.1 shows schematic view of experimental system. The lead annular diaphragms were subject to the uniform initial velocities: 3.5, 8.5, 13.5, 17.44 and 23.5 m/sec. For every case were reported the results of the final profiles and thickness strains of diaphragms. In case of 13.5 m/sec initial velocity, high-speed photographic recordings were

obtained, so that the transient displacements of the diaphragm should be compared with numerical results.

4. CALCULATION CONDITIONS

4.1 Geometry and Processor

The calculation geometries were prescribed and discretized only for the deformable part of the actual diaphragm as shown in Fig.2. The axisymmetric thin shell processor was applied for the diaphragms. Since the shell structure is not discretized in the direction of thickness in this processor, the variation of the principal stress through the thickness is not considered in itself. However, the stress resultants and bending moments are evaluated by integrating with a few Gaussian points through the shell thickness. Therefore, full elastic-plastic deformation can be calculated by this processor.

4.2 Initial and Boundary Conditions

In correspondence with the experimental conditions, the same uniform initial velocities are applied to shell segments. The outer edge of the shell diaphragm is clamped rigidly.

4.3 Material Model

In the reference experiments are included fortunately the results for five different initial velocities. Therefore, consideration of the strain-rate dependency of yield stress leads to good demonstration to indicate the effect of deformation rate on the mechanical behavior.

Since both static and dynamic yield stress are employed and evaluated in the present calculations, kinematical change of deformation is clearly understood by direct comparison of these obtained results.

In the benchmark analyses of the cask drop tests were efficiently discussed and investigated the appropriate forms of constitutive equation for lead even with the strain-rate taken into account (Aizawa, 1988). In actual computation, the calculated starin-rates often exceed beyond 10^2/ sec. Then, the modified Robinson's law is employed for the diaphragms as a proper constitutive equation, where the yield stress is given by

$$\sigma = A \cdot (1 + B \cdot \log_{10} \dot{\varepsilon}) \cdot \varepsilon^n$$

in which ε and $\dot{\varepsilon}$ are the total equivalent strain and strain-rate, respectively. Here, A, B and n are material properties, for pure as-cast lead materials, which are provided by

$$A = 3.92 \text{ [MPa]}, \quad B = 0.096 \text{ [-]}, \quad n = 0.31 \text{ [-]}$$

Here to be noted is the second term of the Robinson's law, which becomes negative value for $\dot{\varepsilon} < 1$ / sec. Then, it might be better that this Robinson's law should be applied to computations when $\dot{\varepsilon} > 1$ /sec, while the static yield stress should be employed for $\dot{\varepsilon} < 1$ /sec.

In the following calculations, material properties other than the dynamic yield stress are assumed by:

Density:	11.3 [g/cm^3]
Young's modulus:	7100 [MPa]
Poisson's ratio:	0.42
Static yield stress:	15.3 [MPa]

5. DISCUSSION OVER IMPACT FORMING OF SHELLS

Fig.3 compares the final displacements of the diaphragms between the calculation and experiment for five different initial velocities. Two kinds of material models are employed in computations: one model independent of strain rate (abbr. SRI) and the other dependent on strain rate (abbr. SRD). The calculated results by SRD are in good agreement with the experimental data irrespective of the intial velocities. In the low initial velocity region little difference is observed between SRI and SRD, while the central part of diaphragm is deformed larger in the petaloid shape for SRI model in the high velocity region. This might be the strain-rate effect: $\dot{\varepsilon}$ exceeds 10^3/sec in the early stage of computation when V=23.5 m/sec, while $\dot{\varepsilon}$ becomes at most 10^2/sec when V=3.5 m/sec. Why only the central part is shaped like a petal may be that $\dot{\varepsilon}$ is always larger than that in the circumferential parts. In Fig.4 are shown the thickness strain $\ln(T_0/T)$ distributions in the radial direction: T_0 and T denote the initial and final thickness of diaphragm, respectively. It should be noted that the thickness strain increases abruptly in the vicinity of the clumped edge for SRI modeling with 23.5 m/sec.

In Fig.5 and 6 are shown the transient profiles of geometry when V=13.5 m/sec, the calculated results by SRI and SRD models are compared with experimental data, respectively. Although the experimental data were not recorded at exactly regular intervals of time, they can help us to understand the deformation behavior. In calculating the time interval: τ when the diaphragm continues to deform, τ for SRI is delayed by 0.2 msec behind the experimentally measured data. While τ for SRD is in agreement with the experimental data.

From the view point of impact or explosive forming, it is interesting to comprehend the geometric effect of a perforate to the total deformation behavior. In Fig.7 are shown the impact deformation behaviors of the annular and the circular diaphragms. The broken and solid lines denote the transient profiles of the circular and the annular diaphragms, repectively. V=13.5 m/sec is assumed as the initial velocity and SRD model is used for both cases. Since the annular diaghragm is more flexible, the total amount of deformation becomes larger and is shaped as the truncated corn-shell panel in the final stage.

6. CONCLUSIONS

Through the present study, we have found :

a) For the impact velocties which exceed 10 m/sec, the strain-rate has significant effect on the deformation behavior of the annular lead diaphragm.

b) A proper constitutive equation with the strain-rate effect taken into account is necessary to estimate the time history of the annular diaphragm deformation.

c) The strain-rate effect appears in the elongation (thickness strain) near the clamped part of the annular diaphragm.

Through these calculations we have concluded that the impact formig phenomena can be simulated by AUTODYN-2D with use of appropriate model, and that thin shell processor in AUTODYN-2D should be adaptive to impact analysis of metal sheet materials in plastic forming.

REFERENCES

Aizawa, T., Ohtubo, H., Yagawa, G., Takeda, H., Toi, Y. (1988) Round robin benchmark tests of impact transient calculations of shipping cask vessels. Impact: Effects of Fast Transient Loadings(Ed. Ammann, W.J. et al), A.A.Balkema, Rotterdam, pp.287-316.

Birnbaum, N.K., Cowler, M.S., Itoh, M., Katayama, M., Obata, H. (1987).

AUTODYN-An interactive non-linear dynamic analysis program for microcomputers through supercomputers. Trans. 9th SMiRT Conf., Vol B, pp.401-406.

Birnbaum, N.K., Cowler, M.S., Itoh, M., Katayama, M., Obata, H., Kurobe, A. (1987). Non-linear dynamic analysis of missile impact with experimental verification. Trans. 9th SMiRT Conf., Vol J, pp.127-132.

Ghosh, S.K., Travis, F.W. (1985). On the Large Plastic Deformation of Clamped Annular Diaphragms Under Impulsive Loading. Metal Forming and Impact Mechanics(Ed. Reid, S.R.), Pergamon Press, pp.195-212.

Itoh, M, Cowler, M.S. (1987). An interactive Lagrangian approach to two dimensional penetration analysis. Trans. 9th SMiRT Conf., Vol B, pp.101-106.

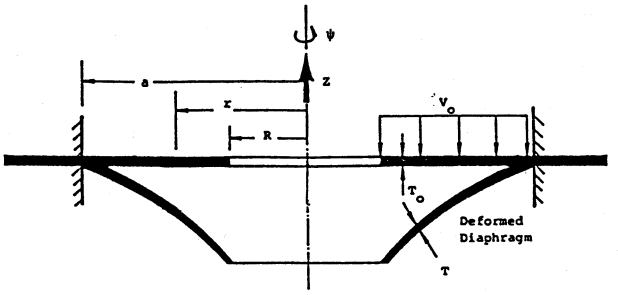

Fig.1 Schematic view of the experimental system

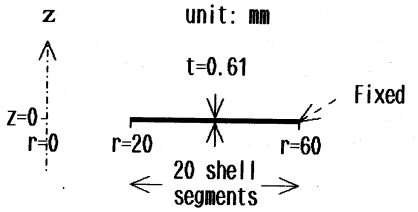

Fig.2 Calculation geometries

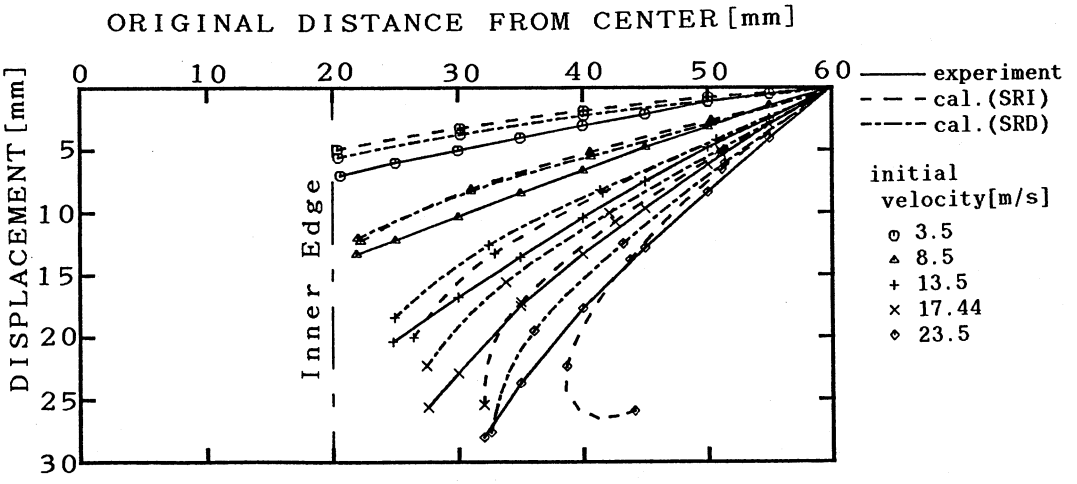

Fig. 3 Comparison of final displacements

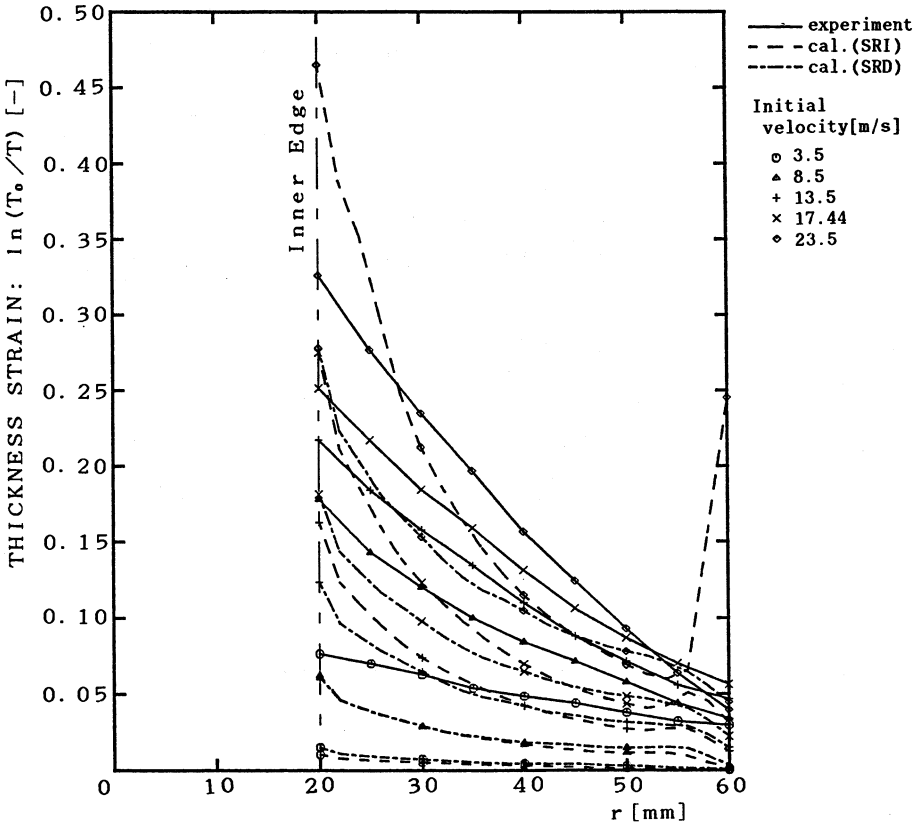

Fig. 4 Comparison of calculated and experimental thickness strain distributions

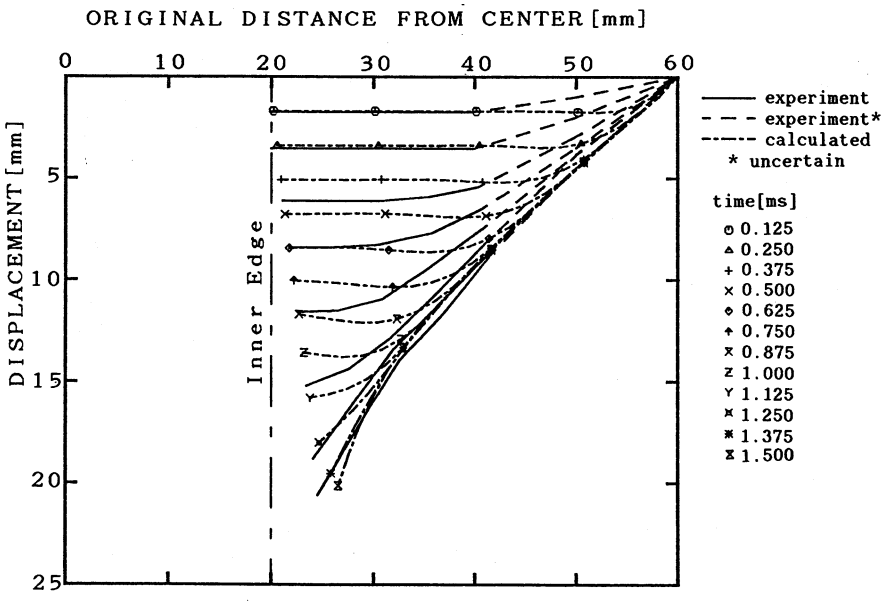

Fig. 5 Comparison of transient profiles between experiment and SRI

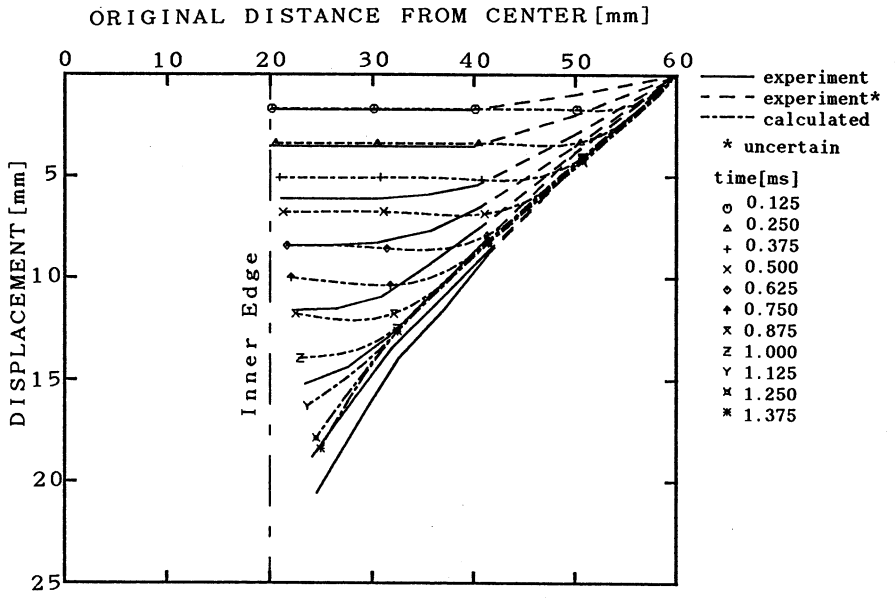

Fig. 6 Comparison of transient profiles between experiment and SRD

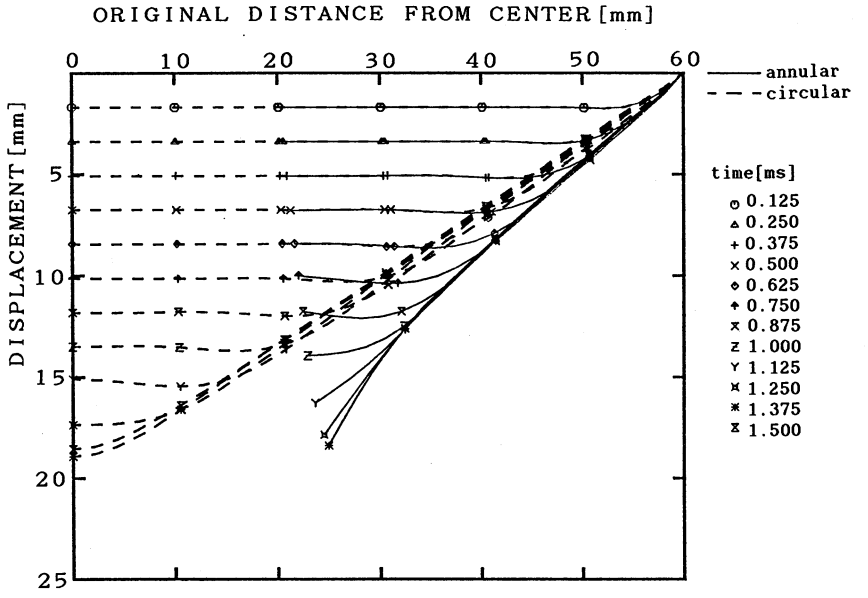

Fig. 7 Comparison of calculated transient profiles between annular and circular diaphragms